Phys. Status Solidi RRL **10**, No. 1, 68–74 (2016) / **DOI** 10.1002/pssr.201510163

Part of Focus Issue on
Carbononics
Eds.: Pawel Hawrylak, Francois Peeters, Klaus Ensslin

pss +++rapid research letters+++
www.pss-rapid.com

Review@RRL

The importance of edges in reactive ion etched graphene nanodevices

Dominik Bischoff*, Pauline Simonet, Anastasia Varlet, Hiske C. Overweg, Marius Eich, Thomas Ihn, and Klaus Ensslin

Solid State Physics Laboratory, ETH Zurich, Otto-Stern-Weg 1, 8093 Zurich, Switzerland

Received 15 May 2015, revised 8 August 2015, accepted 17 August 2015
Published online 27 August 2015

Keywords graphene, nanoribbons, quantum dots, edges, disorder

* Corresponding author: e-mail dominikb@phys.ethz.ch

Patterned graphene nanodevices are promising candidates for nano- and quantum-electronics. Low temperature electronic transport in reactive ion etched graphene nanodevices is typically governed by charge localization manifesting itself in the appearance of Coulomb blockade. The disorder originating from non-perfect graphene edges was identified as being the dominant reason for the stochastic charge localization in graphene nanoribbons. It was found that electrons can localize along the edges on length scales much longer than the physical disorder length. Such states localized along the edge can even leak out of the nanoribbon into adjacent wide graphene leads suggesting that a possibly existing confinement gap is not required to explain transport properties of etched graphene nanodevices. These insights are then used to improve the understanding of transport in graphene quantum dots where Coulomb blockade is typically more regular than in nanoribbons. It is shown that non-overlapping Coulomb diamonds can be observed even in a regime where three states of localized charge need to be passed in series by an electron traveling from source to drain contact. This counter-intuitive observation is explained by higher order co-tunneling through the localized states in the nanoribbons connecting the graphene dot to the leads.

1 Introduction Graphene – a single layer of carbon atoms covalently bonded to each other – is a unique material with extraordinary properties [1, 2]. The low resistance, high tunability and long elastic mean free path together with a special band structure make it a promising material for future applications. As pristine graphene does not possess a band gap, it cannot directly be used in existing nanoelectronic device designs. It was predicted by theory that narrow graphene stripes called nanoribbons can exhibit a band gap as well as other interesting properties such as edge states [3, 4]. By connecting a graphene island to graphene leads via such nanoribbons, quantum dot devices can be fabricated [5, 6]. Graphene quantum dots were predicted to exhibit long spin lifetimes due to low spin–orbit and hyperfine coupling [7–9] which would make them valuable components for quantum information processing.

Over the last years, many different techniques were used to pattern graphene nanodevices for electronic transport experiments. Employed technologies include etching of lithographically patterned devices with plasma [10, 11], etching of devices using nanowires as masks [12], unzipping of carbon nanotubes [13, 14], bottom-up fabrication

from molecules [15], growth on silicon carbide step edges [16, 17] and various others. This review focuses on devices defined by a lithography process and subsequent etching with a plasma process such as reactive ion etching (RIE). This approach allows to fabricate devices with nearly arbitrary geometry.

By performing electronic transport experiments on RIE patterned devices, it was found that the conductivity is generally reduced compared to micron-sized devices and often strongly suppressed around the charge neutrality point [10, 11]. The origin of this suppressed conductance was first attributed to the opening of a band gap predicted by theory [10, 11]. Later experiments clearly observed Coulomb blockade [18–23] in graphene nanoribbons at sufficiently low temperatures indicating that transport is governed by localized charges. Figure 1a shows the conductance for a typical graphene nanoribbon as a function of applied back-gate voltage (or equivalently charge carrier density) and Fig. 1b as a function of applied bias voltage.

1.1 Structure of this review In Section 2, different imperfections in graphene nanodevices are discussed with the aim of identifying the parameters limiting transport properties in state-of-the-art devices. Based on this discussion, in Section 3 areas and locations are estimated on which charges are localized in graphene nanoribbons. This knowledge is then used to develop a qualitative picture of charge transport through a graphene quantum dot in Section 4. Finally, the findings from this review are summarized in Section 5, and Section 6 provides a short outlook of possible future experiments.

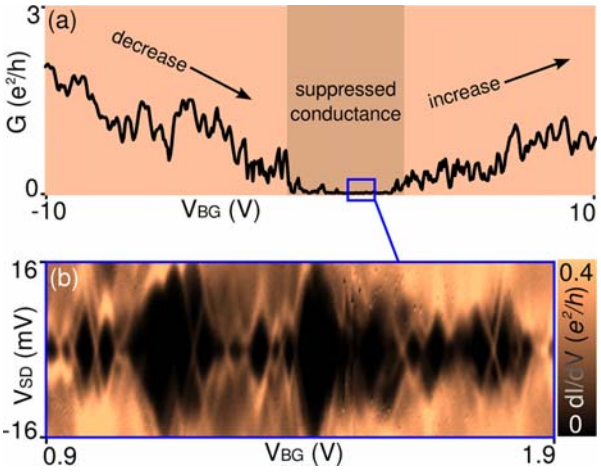

Figure 1 (a) Conductance of a 80 nm wide and 240 nm long graphene nanoribbon. As a function of applied back-gate voltage (or equivalently charge carrier density), the conductance typically decreases non-monotonically (hole regime) until it reaches a region of suppressed conductance. At higher voltages, the conductance increases again (electron regime). (b) Conductance as a function of applied back-gate voltage and source-drain voltage in the region of suppressed conductance marked in blue in (a). Stochastically distributed Coulomb blockade diamonds are observed. (Data of device #2 from Ref. [24].)

2 Bulk versus edge disorder There are many imperfections in etched graphene nanodevices that could be responsible for the random charge localization, therefore preventing the observation of quantized conductance in graphene nanoribbons predicted by theory [25–27]. These imperfections can be grouped into two categories: bulk effects and edge effects. Bulk effects include the environment such as substrate imperfections [28], fabrication residues [29] and lattice defects [30]. Edge effects include microscopically rough edges, molecules bound to the edge [31], edge reconfigurations [32] and edges not following the primary crystallographic orientations [33]. A selection of these effects is shown in Fig. 2 where bulk imperfections are highlighted in blue and edge imperfections are highlighted in red. In order to improve transport properties of graphene nanodevices, it is crucial to determine the imperfections that result in the observed charge localization.

While it is so far technologically challenging to controllably alter the graphene edges, it was shown that the influence of bulk effects can be significantly reduced by fabricating graphene devices on a hexagonal boron nitride (hBN) substrate and a subsequent cleaning step by thermal annealing [34]. This improvement in device fabrication was used to fabricate both graphene nanoribbons as well as micron-sized control devices on hBN [24]. All the devices were fabricated from the same graphene flake in close vicinity to each other. While a significant improvement of transport properties (mobility, disorder density) was found for micron-sized control devices, the electronic properties of ribbons on hBN were indistinguishable from their counterparts fabricated on traditional silicon dioxide substrates [24]: conductance is still suppressed around the charge neutrality point due to the localization of charge carriers leading to Coulomb blockade. From these results it can be concluded that the imperfect edges in reactive-ion etched

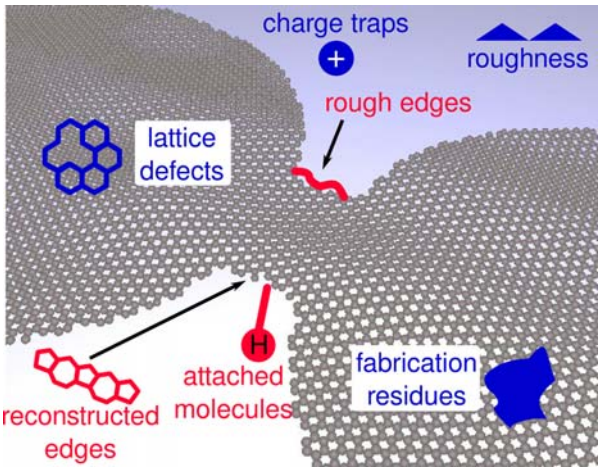

Figure 2 Illustration of a number of different disorder types. Disorder sources originating from the edge are labeled in red and disorder sources related to the bulk of the graphene, the substrate or the environment are colored in blue.

graphene nanodevices are mainly responsible for the observed charge localization.

To further test this hypothesis, the devices were contaminated with a polymer used for the lithography step: the transport properties of the control devices deteriorated notably while no clear change was observed for the ribbon devices [24]. This is in line with the argument that disorder from the edge is dominant.

Smith et al. [35] extended this approach by evaporating cesium atoms on top of their nanoribbons fabricated on silicon dioxide. A pronounced shift of the charge neutrality point and a broadening of the region of suppressed conductance were found. The doping was explained by charge transfer from the metal atoms to the graphene. The enhanced suppression of conductance suggested that bulk disorder can indeed influence transport in graphene nanodevices.

The different outcome of the two experiments [24, 35] suggests that as long as bulk disorder is weak, mainly edge disorder is responsible for charge localization. By introducing strong short-range disorder via the metal atoms, charge carriers can likely be localized around these atoms.

3 Charge localization along the edge Short nanoribbons with a length of only 30 nm were fabricated on a hBN substrate to reduce the length of edges that were found to be responsible for charge localization [36]. Compatible with previous experiments, Coulomb blockade diamonds were observed. By analyzing the width ΔV_{BG} of the Coulomb diamonds, the capacitance between the area on which charge is localized and the back gate can be estimated: $C_{loc,BG} \geq e/\Delta V_{BG}$. Assuming that charge carriers are localized in the bulk of the nanoribbon and by carefully converting the capacitances into areas, a puzzling result was obtained: the area on which charge is localized can be up to ten times larger than the nanoribbon itself [36].

Coulomb blockade is observed when an electron tunnels from one of the leads into the localized state and then out again into the other lead. Additionally, the localized state needs to connect the delocalized wave functions in the two wide graphene leads therefore enabling current to flow.

It is clear that a band/confinement gap alone cannot explain charge localization on an area larger than the constriction as no seizable gap is expected in the graphene leads. Along similar lines, models suggesting the combination of a confinement gap and some background disorder potential [22, 23, 37, 38] are not able to explain the results. Even if a mechanism could be found that localizes the electrons in the nanoribbon and its closer vicinity, a large wave function overlap between delocalized states in the leads and the localized state in the nanoribbon (yellow, Fig. 3a) would likely result in strong coupling and therefore prevent tunneling. This situation is schematically depicted in Fig. 3a.

Figure 3b presents the solution suggested to solve this puzzle [36]: charge carriers could be primarily localized along the edge of the device and are allowed to extend out of the nanoribbon along the edge of the graphene leads. Along the edge, the capacitance to the back gate is enhanced due to electrostatic stray fields resulting in a locally higher capacitance and therefore an apparently larger area. Additionally, the small wave-function overlap between the two-dimensional delocalized states in the leads and the quasi-one-dimensional states along the edge should allow for tunneling. Notably, the length scales on which charge is localized along the edge ($\approx$100 nm) are much larger than the physical disorder length ($\approx$1 nm). It is therefore unlikely that the states contributing to transport are localized around single defect sites.

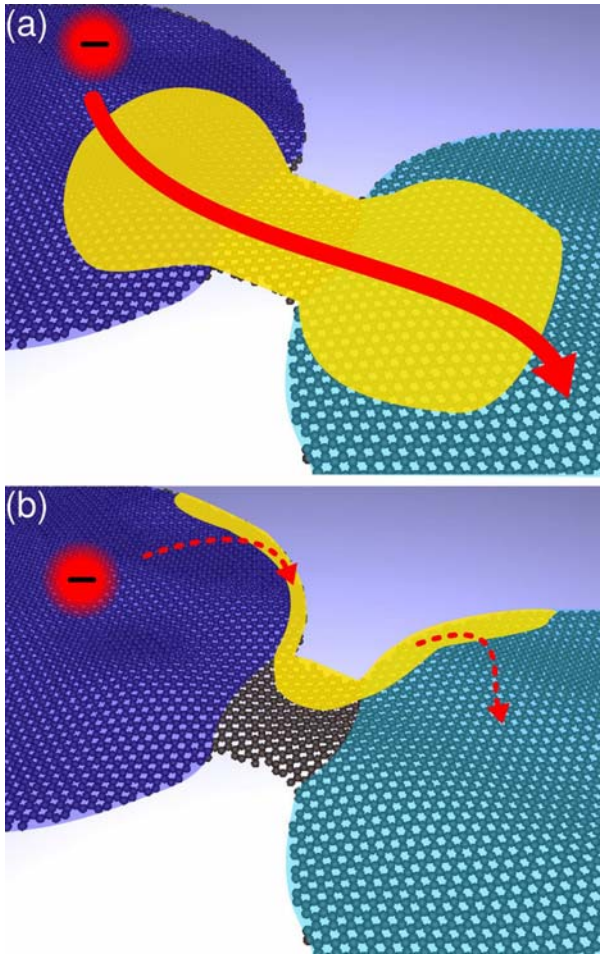

Figure 3 (a) Schematic of a graphene nanoribbon with a possible wave function envelope of a localized state (yellow) and wave function envelopes of delocalized states in the adjacent graphene leads (blue). Due to the large expected overlap of the wave functions, the resulting strong coupling will likely prevent tunneling from the blue states into the yellow state. It is therefore unlikely that Coulomb blockade could be observed. (b) If the wave function of the localized state is primarily situated at the edge of the device, a small wave function overlap might result in tunneling between the delocalized states in the leads and the localized state in the nanoribbon that extends along the edge of the device. In such a case the observation of Coulomb blockade might be possible.

The exact mechanism for the localization along the edge is currently not understood. As a huge variety of devices fabricated by different processes (e.g. Refs. [18–21, 39, 40]) show charge localization, the exact type of edge disorder is probably unimportant as long as it is sufficiently strong. Qualitatively, one can argue that an edge in graphene is equivalent to a surface in a three-dimensional crystal where it is well known that symmetry breaking can result in surface states [41]. It is therefore plausible that localized states exist at disordered graphene edges.

4 Localization in graphene quantum dots The insights about graphene nanoribbons are next applied to graphene quantum dots. Graphene quantum dots fabricated by RIE typically consist of a graphene island that is connected via two nanoribbons to two wide graphene leads [5, 6]. Therefore, it could be expected that a graphene quantum dot would show even more irregular Coulomb blockade diamonds as an electron moving through the structure has to pass through two ribbons and an island. This is however not what is typically observed in experiment: most graphene quantum dots show rather regular Coulomb blockade diamonds closing at small bias [5, 6, 42–44]. In order to understand this behavior better, it is necessary to determine where charges are localized as well as which transport mechanisms lead to these significantly more regular Coulomb blockade diamonds.

In Ref. [45], a bilayer graphene quantum dot with a geometry depicted schematically in Fig. 4a was investigated. It was found that measurements of the current strongly depended on the choice of side gate voltages that were varied: sweeping one of the left gates (L) versus one of the right gates (R) resulted in current patterns showing three distinct sets of lines as exemplarily shown in Fig. 4b. The observed lines show avoided crossing indicating strong coupling between individual states of localized charge. This data suggest that at least three sites of localized charges are present in the system [45]. While the diagonal lines are about equally spaced, the other two sets are not (see light blue lines), indicating energy dependent geometries of the involved localized states.

The situation is different when using only both left (or only both right) gates as exemplarily shown in Fig. 4c: only one set of lines is visible [45]. This does, however, not imply that only one site of localized charge is present but rather that all sites couple equally well to both employed side gates. Using all combinations of side gates, it was possible to roughly triangulate the positions where localized charges were situated: one site must be located in the island and one site each somewhere close to or in the nanoribbons [45]. This situation is depicted in Fig. 5a.

When measuring the current flowing through the dot as a function of applied bias, Coulomb diamonds are observed [45] as shown in Fig. 6. In contrast to the measurement presented in Fig. 1b for a graphene nanoribbon, the diamonds are much more regular and most of them close at low bias voltage. This is exactly the behavior expected for

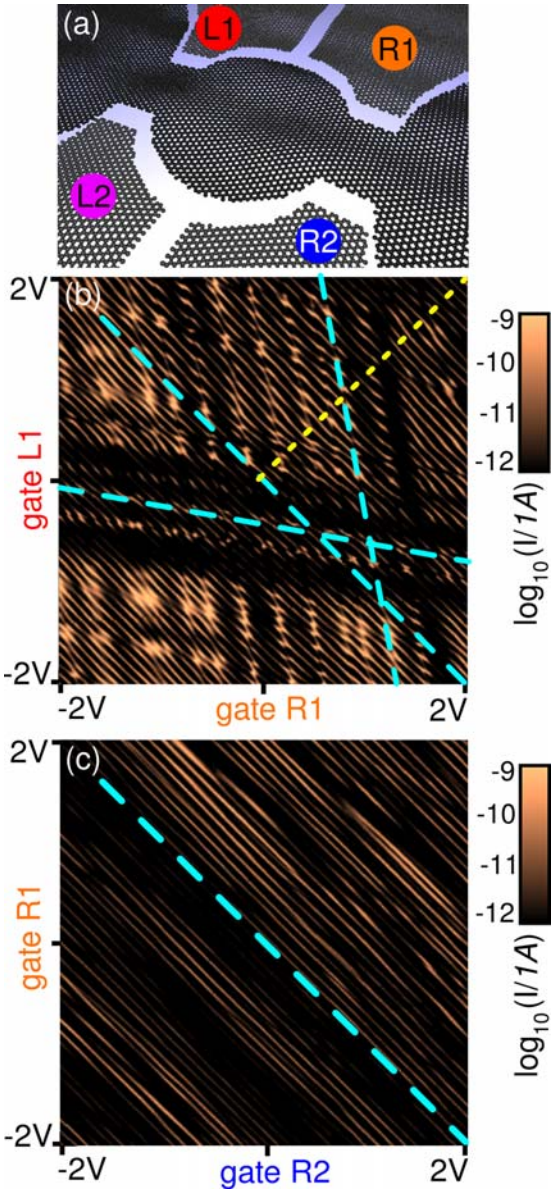

Figure 4 (a) Schematic drawing of the investigated device: a bilayer graphene quantum dot with 4 lateral side gates L1/2 and R1/2. (b) Current flowing through the quantum dot measured at small bias as a function of gates L1 and R1. Three different sets of lines are visible as highlighted by the blue dashed lines. Clear avoided crossings between different sets of lines can be observed. (c) Current flowing through the dot as a function of R1 and R2. Here, only one set of lines is visible. (Same data as published in Ref. [45].)

a single quantum dot and not expected for three dots in series. This apparent contradiction can be resolved by taking co-tunneling into account, which is a higher order tunneling process via virtual intermediate states. The higher the order of the co-tunneling process is, the lower is generally the probability for it to happen [46, 47]. For a system with three dots in series, the following combinations can occur: normal tunneling (all three levels aligned with leads), sec-

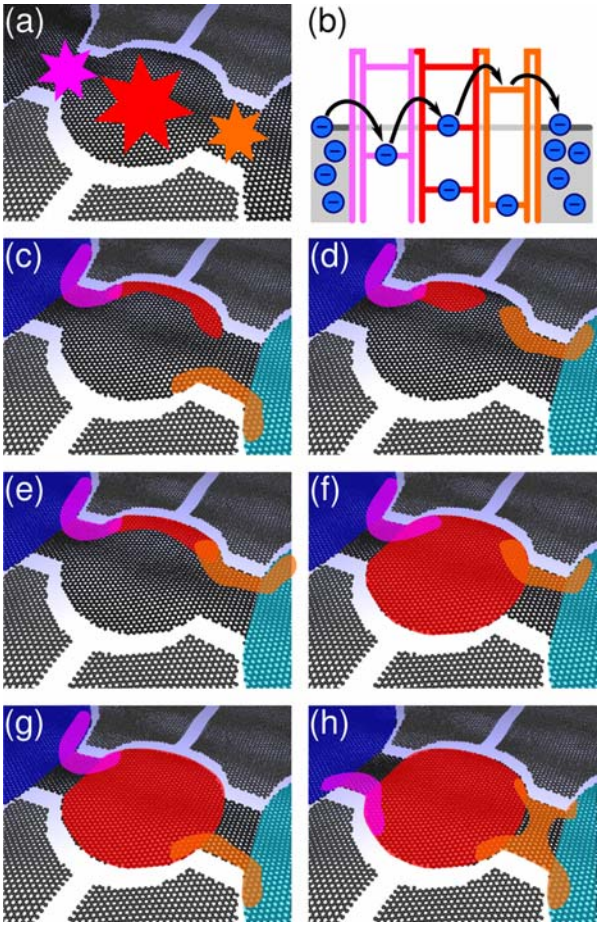

Figure 5 (a) Schematic position of the states of localized charge for the experiment in Figs. 4 and 6 (see also Refs. [36, 45]). (b) Cotunneling process resulting in current through a serial triple quantum dot: in order to enter the middle dot which is aligned with the leads, electrons need to go via virtual states in the outer two dots. (c, d) Schematic drawing of two possible sets of wave function envelopes that will not contribute to current. (e) Set of wave function envelopes that will contribute to current but fail to produce the symmetry observed in experiment. (f–h) Possible sets of wave function envelopes that are compatible with the observations of the experiment in Ref. [45].

ond order co-tunneling (two levels aligned), two times second order co-tunneling (only middle level aligned), third order co-tunneling (one of outer levels aligned) or fourth order co-tunneling (none of the levels aligned). As a triple dot system has a three-dimensional parameter space, the most common case is that either zero or one of the levels are aligned with the leads. As a consequence, current is more likely to flow when the middle level is aligned than when one of the outer levels is aligned. This results in the regular observed Coulomb blockade diamonds originating from the charge localized on the island. This situation where the outer dots act as tunneling barriers via higher order co-tunneling processes is depicted in Fig. 5b. Equivalently, the system can be understood as a coherently coupled triple dot molecule.

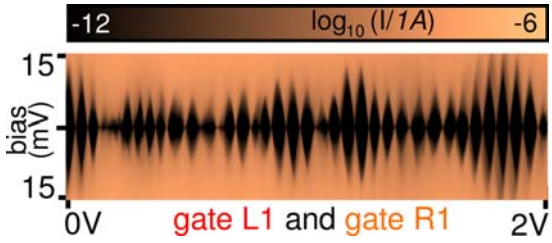

Figure 6 Coulomb blockade diamonds recorded along the yellow dashed line in Fig. 4b. (Same data as published in Ref. [45].)

Next, possible wave function envelopes are discussed. Many combinations of wave function envelopes will not contribute to the current as schematically depicted in Fig. 5c, d since they fail to connect the two leads. Others, as for example the one shown in Fig. 5e, will not fulfill the observed symmetry as the red state of localized charge is much stronger coupled to the upper gates than to the lower gates. This is in principle also true for the states in the ribbons, but due to the geometry of the investigated device, it is unlikely that a state on one ribbon edge could be experimentally discerned from a state at the other ribbon edge. It is therefore clear that in order to fulfill all requirements, the wave function of the state in the dot needs to be extended over the whole island as depicted in Fig. 5f–h. This extension over the whole island consequently results in the quite regular Coulomb blockade diamonds observed experimentally and is compatible with the capacitance obtained from the width of the Coulomb blockade diamonds.

5 Conclusion It was shown that disordered edges in etched graphene nanostructures are currently the main origin of the charge localization observable as Coulomb blockade in electronic transport measurements. By carefully analyzing capacitances of localized states in ultrashort nanoribbons, it was suggested that electrons can be localized along the edges of a device on length scales much longer than the physical disorder length. These edge states can continue along the edge in the wider lead parts of the device. This indicates that a potential band/confinement gap is not the relevant mechanism for the observed suppression of conductance around the charge neutrality point. As an edge always breaks the symmetry of the crystal, it is not surprising to find electronic states localized along the edge – similar to surface states in three-dimensional crystals.

By comparing graphene nanoribbons with graphene quantum dots, it was found that dot geometries usually feature more regular Coulomb blockade diamonds despite being built of two nanoribbons and an island in series. By careful triangulation of the sites of localized charge, it was found that localized states exist in each of the constrictions, as expected. Further, one state was found to be delocalized over the actual dot structure. By taking into account higher order co-tunneling processes, the following picture was suggested: the observed regular Coulomb blockade diamonds belong to the state being extended over the whole

island. Transport to and from this island happens via cotunneling through localized states in the nanoribbons.

A more detailed and technical review of this line of research can be found in Ref. [48].

6 Perspectives There are many open questions concerning the exact extent of wave functions or the microscopic origins of the charge localization along the edge. More insight into those questions could be obtained by combining scanning tunneling microscopy together with low temperature transport experiments. It might also be worthwhile to further investigate chemical functionalization of edges [31, 49] in order to obtain smoother potentials.

Alternatively, novel device designs can be investigated. A promising approach is the electrostatic definition of quantum dot structures in bilayer graphene [50, 51]. It would further be possible to replace the nanoribbons defining the connections to the island by real tunneling barriers: a graphene island could be separated from conducting electrodes via a two-dimensional insulator such as hBN or WS_2 [52, 53].

Acknowledgements Financial support by the National Center of Competence in Research on Quantum Science and Technology (NCCR QSIT) funded by the Swiss National Science Foundation, by the Marie Curie ITNs S^3NANO and QNET is gratefully acknowledged.

References

[1] K. S. Novoselov, A. K. Geim, S. V. Morozov, D. Jiang, Y. Zhang, S. V. Dubonos, I. V. Grigorieva, and A. A. Firsov, Science **306**, 666–669 (2004).
[2] A. K. Geim and K. S. Novoselov, Nature Mater **6**, 183–191 (2007).
[3] K. Nakada, M. Fujita, G. Dresselhaus, and M. S. Dresselhaus, Phys. Rev. B **54**, 17954–17961 (1996).
[4] M. Fujita, K. Wakabayashi, K. Nakada, and K. Kusakabe, J. Phys. Soc. Jpn. **65**, 1920–1923 (1996).
[5] C. Stampfer, J. Güttinger, F. Molitor, D. Graf, T. Ihn, K. Ensslin, Appl. Phys. Lett. **92**, 012102 (2008).
[6] L. A. Ponomarenko, F. Schedin, M. I. Katsnelson, R. Yang, E. W. Hill, K. S. Novoselov, A. K. Geim, Science **320**, 356–358 (2008).
[7] B. Trauzettel, D. V. Bulaev, D. Loss, and G. Burkard, Nature Phys. **3**, 192–196 (2007).
[8] P. Recher and B. Trauzettel, Nanotechnology **21**, 302001 (2010).
[9] M. Fuchs, J. Schliemann, and B. Trauzettel, Phys. Rev. B **88**, 245441 (2013).
[10] Z. Chen, Y.-M. Lin, M. J. Rooks, and P. Avouris, Physica E **40**, 228–232 (2007).
[11] M. Y. Han, B. Özyilmaz, Y. Zhang, and P. Kim, Phys. Rev. Lett. **98**, 206805 (2007).
[12] J. Bai, X. Duan, and Y. Huang, Nano Lett. **9**, 2083–2087 (2009).
[13] L. Jiao, L. Zhang, X. Wang, G. Diankov, and H. Dai, Nature **458**, 877–880 (2009).
[14] D. V. Kosynkin, A. L. Higginbotham, A. Sinitskii, J. R. Lomeda, A. Dimiev, B. K. Price, and J. M. Tour, Nature **458**, 872–877 (2009).
[15] J. Cai, P. Ruffieux, R. Jaafar, M. Bieri, T. Braun, S. Blankenburg, M. Muoth, A. P. Seitsonen, M. Saleh, X. Feng, K. Müllen, and R. Fasel, Nature **466**, 470–473 (2010).
[16] J. Baringhaus, M. Ruan, F. Edler, A. Tejeda, M. Sicot, A. Taleb-Ibrahimi, A.-P. Li, Z. Jiang, E. H. Conrad, C. Berger, C. Tegenkamp, and W. A. de Heer, Nature **506**, 349–354 (2014).
[17] M. S. Nevius, F. Wang, C. Mathieu, N. Barrett, A. Sala, T. O. Mentes, A. Locatelli, and E. H. Conrad, Nano Lett. **14**, 6080–6086 (2014).
[18] B. Özyilmaz, P. Jarillo-Herrero, D. Efetov, and P. Kim, Appl. Phys. Lett. **91**, 192107 (2007).
[19] X. Liu, J. B. Oostinga, A. F. Morpurgo, and L. M. K. Vandersypen, Phys. Rev. B **80**, 121407 (2009).
[20] S. Masubuchi, M. Ono, K. Yoshida, K. Hirakawa, and T. Machida, Appl. Phys. Lett. **94**, 082107 (2009).
[21] F. Molitor, A. Jacobsen, C. Stampfer, J. Güttinger, T. Ihn, and K. Ensslin, Phys. Rev. B **79**, 075426 (2009).
[22] C. Stampfer, J. Güttinger, S. Hellmüller, F. Molitor, K. Ensslin, and T. Ihn, Phys. Rev. Lett. **102**, 056403 (2009).
[23] K. Todd, H.-T. Chou, S. Amasha, and D. Goldhaber-Gordon, Nano Lett. **9**, 416–421 (2009).
[24] D. Bischoff, T. Krähenmann, S. Dröscher, M. A. Gruner, C. Barraud, T. Ihn, and K. Ensslin, Appl. Phys. Lett. **101**, 203103 (2012).
[25] D. Gunlycke, D. A. Areshkin, and C. T. White, Appl. Phys. Lett. **90**, 142104 (2007).
[26] D. A. Areshkin, D. Gunlycke, and C. T. White, Nano Lett. **7**, 204–210 (2007).
[27] T. C. Li and S.-P. Lu, Phys. Rev. B **77**, 085408 (2008).
[28] J. Xue, J. Sanchez-Yamagishi, D. Bulmash, P. Jacquod, A. Deshpande, K. Watanabe, T. Taniguchi, P. Jarillo-Herrero, and B. J. LeRoy, Nature Mater. **10**, 282–285 (2011).
[29] J. Moser, A. Barreiro, and A. Bachtold, Appl. Phys. Lett. **91**, 163513 (2007).
[30] J.-H. Chen, W. G. Cullen, C. Jang, M. S. Fuhrer, and E. D. Williams, Phys. Rev. Lett. **102**, 236805 (2009).
[31] T. Kato, L. Jiao, X. Wang, H. Wang, X. Li, L. Zhang, R. Hatakeyama, and H. Dai, Small **7**, 574–577 (2011).
[32] P. Koskinen, S. Malola, and H. Häkkinen, Phys. Rev. B **80**, 073401 (2009).
[33] X. Jia, M. Hofmann, V. Meunier, B. G. Sumpter, J. Campos-Delgado, J. M. Romo-Herrera, H. Son, Y.-P. Hsieh, A. Reina, J. Kong, M. Terrones, and M. S. Dresselhaus, Science **323**, 1701–1705 (2009).
[34] C. R. Dean, A. F. Young, I. Meric, C. Lee, L. Wang, S. Sorgenfrei, K. Watanabe, T. Taniguchi, P. Kim, K. L. Shepard, and J. Hone, Nature Nano **5**, 722–726 (2010).
[35] C. W. Smith, J. Katoch, and M. Ishigami, Appl. Phys. Lett. **102**, 133502 (2013).
[36] D. Bischoff, F. Libisch, J. Burgdörfer, T. Ihn, and K. Ensslin, Phys. Rev. B **90**, 115405 (2014).
[37] P. Gallagher, K. Todd, D. Goldhaber-Gordon, Phys. Rev. B **81**, 115409 (2010).
[38] F. Molitor, C. Stampfer, J. Güttinger, A. Jacobsen, T. Ihn, and K. Ensslin, Semicond. Sci. Technol. **25**, 034002 (2010).

[39] T. Kato and R. Hatakeyama, Nature Nano **7**, 651–656 (2012).
[40] D.-K. Ki and A. F. Morpurgo, Phys. Rev. Lett. **108**, 266601 (2012).
[41] C. Kittel, Einführung in die Festkörperphysik, Vol. 14 (Oldenburg Verlag, München, Wien, 2006), pp. 181–206.
[42] J. Güttinger, C. Stampfer, S. Hellmüller, F. Molitor, T. Ihn, and K. Ensslin, Appl. Phys. Lett. **93**, 212102 (2008).
[43] L.-J. Wang, G. Cao, T. Tu, H.-O. Li, C. Zhou, X.-J. Hao, Z. Su, G.-C. Guo, H.-W. Jiang, and G.-P. Guo, Appl. Phys. Lett. **97**, 262113 (2010).
[44] S. Fringes, C. Volk, C. Norda, B. Terres, J. Dauber, S. Engels, S. Trellenkamp, and C. Stampfer, Phys. Status Solidi B **248**, 2684–2687 (2011).
[45] D. Bischoff, A. Varlet, P. Simonet, T. Ihn, and K. Ensslin, New J. Phys. **15**, 083029 (2013).
[46] S. De Franceschi, S. Sasaki, J. M. Elzerman, W. G. van der Wiel, S. Tarucha, and L. P. Kouwenhoven, Phys. Rev. Lett. **86**, 878–881 (2001).
[47] D. Schröer, A. D. Greentree, L. Gaudreau, K. Eberl, L. C. L. Hollenberg, J. P. Kotthaus, and S. Ludwig, Phys. Rev. B **76**, 075306 (2007).
[48] D. Bischoff, A. Varlet, P. Simonet, M. Eich, H. C. Overweg, T. Ihn, and K. Ensslin, Appl. Phys. Rev. **2**, 031301 (2015).
[49] X. Wang, S. M. Tabakman, and H. Dai, J. Am. Chem. Soc. **130**, 8152–8153 (2008).
[50] M. T. Allen, J. Martin, and A. Yacoby, Nature Commun. **3**, 934 (2012).
[51] A. M. Goossens, S. C. M. Driessen, T. A. Baart, K. Watanabe, T. Taniguchi, and L. M. K. Vandersypen, Nano Lett. **12**, 4656–4660 (2012).
[52] L. Britnell, R. V. Gorbachev, R. Jalil, B. D. Belle, F. Schedin, M. I. Katsnelson, L. Eaves, S. V. Morozov, A. S. Mayorov, N. M. R. Peres, A. H. Castro Neto, J. Leist, A. K. Geim, L. A. Ponomarenko, and K. S. Novoselov, Nano Lett. **12**, 1707–1710 (2012).
[53] T. Georgiou, R. Jalil, B. D. Belle, L. Britnell, R. V. Gorbachev, S. V. Morozov, Y.-J. Kim, A. Gholinia, S. J. Haigh, O. Makarovsky, L. Eaves, L. A. Ponomarenko, A. K. Geim, K. S. Novoselov, and A. Mishchenko, Nature Nano **8**, 100–103 (2013).

